PREPRINT UCRL-79236

Conf-771118--1

Lawrence Livermore Laboratory

PARTICLE-IN-CELL VS STRAIGHT LINE GAUSSIAN CALCULATIONS FOR AN AREA OF COMPLEX TOPOGRAPHY

Rolf Lange
Christine Sherman

MASTER

March 4, 1977

This paper was prepared for presentation at the Conference on Applications of Air Pollution Meteorology sponsored by APCA and AMS, Salt Lake City, Utah, Nov. 1977.

Contents

PARTICLE-IN-CELL VS STRAIGHT LINE GAUSSIAN CALCULATIONS FOR AN AREA OF COMPLEX TOPOGRAPHY*

ABSTRACT

Two numerical models for the calculation of time integrated air concentration and ground deposition of airborne effluent releases are compared. The time dependent Particle-In-Cell (PIC) model and the steady state Gaussian plume model were used for the simulation. The area selected for the comparison was the Hudson River Valley, New York. Input for the models was synthesized from meteorological data gathered in previous studies by various investigators. It was found that the PIC model more closely simulated the three-dimensional effects of the meteorology and topography. Overall, the Gaussian model calculated higher concentrations under stable conditions. In addition, because of its consideration of exposure from the returning plume after flow reversal, the PIC model calculated air concentrations over larger areas than did the Gaussian model.

INTRODUCTION

For a routine airborne release, the concentration of radioactive material in the surrounding region depends on the amount of effluent released; the height of the release; the mementum and buoyancy of the emitted plume; the

*Work performed under the auspices of the U.S. Energy Research & Development Administration under contract No. W-7405-Eng-48 and was supported by the Nuclear Regulatory Commission (NRC), under Work Authorization A0158.

windspeed, atmospheric stability, and airflow patterns of the site, and various effluent removal mechanisms. Geographical features such as hills, valleys, and large bodies of water greatly influence dispersion and airflow patterns.

In this study, we analyzed the differences between calculations of time integrated air concentration and ground deposition for the standard Straight-Line Gaussian Plume Model and the 3-dimensional time dependent PIC model, for a river valley site of complex meteorology and topography. The PIC model used in this study is the Atmospheric Diffusion Particle-in-Cell (ADPIC) computer code.

We chose the Hudson River Valley for the numerical simulation and comparisons because of its complex geography and sea breeze meteorology. We synthesized a regional, 24-h cyclic wind field using data from previous investigations of the wind-flow patterns in this area. We wished to analyze the two models on a regional scale for an assumed operating release in a particular meteorological regime.

II. MODEL DISCUSSION

The straight-line Gaussian plume diffusion calculations were made with the LLL computer code CPS (continuous point source).[1] It is based on the standard Gaussian plume formulation as discussed in Slade.[2] The code outputs time integrated concentrations and deposition in the form of contour plots as a function of azimuth for 16 sectors and as a function of distance from the source.

The PIC model components and the input information required to calculate integrated air concentrations and ground deposition from time-

and space-varying meteorological input data are depicted in Fig. II-1. MEDIC is a meteorological data interpolation computer code used to interpolate multiple horizontal wind measurements to model grid points at a fixed height above topography. WINDY is its input file that contains the suitably time averaged meteorological data sets. Output from MEDIC is used by MATHEW[3,4] to calculate a three-dimensional nondivergent regional windfield. MATHEW is a meteorological adjustment model that provides the diffusion and transport model, ADPIC,[5,6] with mass-consistent, three-dimensional time varying wind fields, which are adjusted by a weighted lease squares method to satisfy the continuity equation within the specified model volume. The upper and lateral boundaries are assumed to be open air, thus allowing mass to flow through these boundaries. The bottom boundary is determined by the topographic elevations of the area of interest.

ADPIC is a hybrid Lagrangian-Eulerian, three-dimensional particle-in-cell code for calculating transport and diffusion of a pollutant from its source to its temporal and regional distribution. This numerical model can simulate transport and diffusion when given speed and directional wind shear, occurrence of calms, space-variable surface roughness, wet and dry deposition, radioactive decay, gravitational settling, space- and time-dependent eddy diffusion parameters, and single or multiple sources of either a continuous or instantaneous nature. ADPIC solves the three-dimensional, advection-diffusion equation in a flux-conservative form, using a pseudovelocity technique in which the advective velocities are supplied by MATHEW, and the diffusive velocities are computed from concentration gradients.

Lagrangian particles represent the pollutant distribution within the structure of the ADPIC grid. The chief advantages of this approach are the virtual elimination of artificial diffusion that is inherent in purely

Eulerian, finite difference codes and the fact that the Langrangian particles can be tagged with their coordinates, mass or size distribution, activity, age, and other properties that might be exhibited by a particular pollutant. In its present form, ADPIC can simulate up to five different species emitted from one location. This allowed us to model simultaneously both noble gases and gases that exhibit a deposition velocity, each with a different half-life.

TOPOG is used to set up the topographical boundary conditions and geographical coordinates for MEDIC, MATHEW, and ADPIC, respectively.

ADPIC has undergone extensive verification against closed solutions to the transport and diffusion equation.[5] In these studies we found that ADPIC results are within 5% of the exact solution for uniform flow fields as well as for wind fields that exhibit vertical wind shear. ADPIC has also been used for plume depletion studies over agricultural land under simple meteorological conditions.[7]

The MATHEW-ADPIC numerical models have been verified against several field tracer studies against several field tracer studies.[6] These studies included methyl-iodine tracer studies at the Idaho National Engineering Laboratory, Idaho, and ^{41}Ar plumes at the Savannah River Plant (SRP), South Carolina. For these studies, the agreement between measurements and calculations has been remarkable consistent; 60% of the calculations are within a factor of two. Measurements were taken at distances of 4 to 80 km from the source and have included high-volume surface samples for the methyl-iodine as well as surface and airborne measurements of gamma energy from ^{41}Ar.

III. MODEL INPUT DATA

Topographic data bases for this study were obtained by averaging fine-resolution elevations supplied by the U.S. Geological Survey for the two areas of interest.

The model-generated topography for the Hudson River Valley calculation consists of a narrow river valley in the north end of the grid with high topography in the west and lower hills toward the east (Fig. III-1). The river narrows into a gorge 200 to 300 m in height. Once through the gorge, the river turns abruptly southwest and begins widening as the topography drops and becomes more rolling. The source release point is slightly southeast of the river gorge, as indicated by the solid circle in Fig. III-1.

The meteorology of the Hudson River Valley site was studied using 2 y of observations at the site itself and in surrounding locations.[8] It was found that, frequently, diurnal valley winds blow up and down the axis of the river valley (up-valley during unstable hours and down-valley during stable hours). We used this information to simulate a diurnal flow regime and to estimate the Pasquill diffusivity categories as a function of the time of day. During transition periods when the flow is reversing, the horizontal diffusion coefficients are larger than during either an up-valley or a down-valley flow. For the vertical diffusion coefficients, we used a stable regime for the nighttime flow conditions, moving into an unstable regime during the daytime hours.

We simulated a cyclic flow reversal in the Hudson River Valley for an early fall, clear weather situation (Fig. III-2). The general flow is characterized by thermally driven currents at the lowest levels with a south to southwesterly flow prevailing above the boundary layer. The nighttime

cycle consists of 14 h of very light (0.25 to 0.5 m/s) northerly flow, gradually increasing to an average of 2.5 m/s as the cool, very stable wedge of drainage air deepens from 20 to 120 m. The daytime cycle consists of a sudden late morning decrease in stability, changing to neutral, to slightly unstable, and then to moderately unstable with a simultaneous breaking up of the thermal inversion, a rapid deepening of the boundary layer, and a quick rise of the southerly wind. An average southerly wind of 3.8 m/s develops for about 6 h with a 2.5 m/s flow existing for 1 h on either end of the cycle. Figure III-3 shows the variation of the inversion height and the mean wind speed as a function of the local time assumed for the calculations in the following section. To input the flow regime into the models, we postulated bogus stations throughout the grid where we input winds that are consistent with the topography and the meteorological conditions under consideration.

In Table III-1 we have listed the three different species used in the model calculations. Two of these are radioactive isotopes, selected because of their relevance to an operating release from a nuclear power reactor. The third, inert gas, was chosen as a control species. All three species were run simultaneously in the ADPIC calculations and were each assumed to be unit rate releases (1 unit/s).

IV MODEL CALCULATIONS

The MATHEW-ADPIC grid for the Hudson River Valley consisted of 38 x 78 x 10 cells of 500 x 500 x 45 m each, giving a total grid block of 19 x 39 x 0.45 km in the east-west, north-south, and vertical directions, respectively. Because the topography protrudes like building blocks into the grid, the

horizontal cell size of 500 m was required to resolve the narrowest part of the river. In the vertical direction, a cell height of 45 m was chosen to give sufficient resolution to the variations in elevation associated with the river valley. Careful consideration was given to the location of the source within the grid. Because ADPIC is a time-dependent code, it was important to ensure sufficient grid space around the source to prevent a significant fraction of the pollutant from escaping the grid before wind reversal occurred and hence the code could model the return of the earlier part of the plume to the source area and beyond.

The wind data were processed hourly with the MEDIC and MATHEW models to produce a three-dimensional, mass-consistent advection field for 24 h. The general features of MEDIC-MATHEW adjustment can be seen through an examination of a sample data set.

The "measured" horizontal wind vectors for 1200 EST are shown in Fig. IV-1. The resulting interpolated horizontal wind in Fig. IV-2a is shown at 90 m above the lowest topography in the grid. The horizontal isotachs are overlaid with streamlines defining the flow direction. The spacing between the streamlines is only qualitatively related to the wind speed. The blank areas in Fig. IV-2 delineate the area where the topography is higher than 90 m above the reference elevation. A comparison of the adjusted horizontal field (Fig. IV-2b) with the interpolated winds (Fig. IV-2a) shows the effect of channeling near the narrowest part of the Valley. The streamline curvature is smoothed and shows more conformity to the terrain. The channeling has also resulted in a 2 m/s increase in a high windspeed area, located one-third of the way from the northern border of the grid. The accompanying vertical velocities for the 90 m level are shown in Fig. IV-3. While the vertical motion is relatively small at this level, it is sufficient to

produce motion over the appropriate terrain features. Where the terrain is more rugged and higher, the wind fields at those levels appropriately show more vertical motion.

Figure IV-4 illustrates another view of the advection field where the horizontal speed and direction are calculated at 45 m above terrain. The relative low speeds are just windward of rising terrain while the relative high speeds occur above the flatter areas.

ADPIC was run for a complete 24 h diurnal cycle. Deposition and integrated surface air concentrations from unit rate surface releases for the three typical reactor effluents were compared with results from the Gaussian model.

The source term consisted of simultaneous, continuous unit rate surface releases of the radioisotopes ^{131}I and ^{138}Xe and the inert gas control species (see Table III-1). The source was assumed to have a Gaussian distribution with a horizontal and vertical standard deviation of σ_H = 10 m and σ_V = 5 m, respectively. Source location was on the edge of the west bank of the river at river level height (Fig. III-1).

The ADPIC code modeled the transport and diffusion of the total pollutant plume by generating some 90,000 tracer particles for a typical 24 h study, of which a maximum of 20,000 resided simultaneously within the grid, the rest either being deposited, radioactively decayed, or carried out of the grid by the diffusion-advection process. The particle-in-cell approach of ADPIC also allows the separate treatment of radioactive decay and deposition of the individual isotopes.

Figures IV-5 to IV-8 give examples of the ADPIC particle distribution, representing the pollutant plume at selected hours. The figures show a projection of the particle distribution on a horizontal plane. The large circle locates the assumed source. The sequence shows the effect of the wind changes (southerly to northerly and back to southerly) on the pollutant transport. Figure IV-5 shows the first wind reversal toward the nighttime drainage regime as the bulk of the pollutant moved southward from the source. The trail of particles north of the source indicates that at upper levels, the wind was still blowing from the south. Figures IV-6 gives a good indication of the influence of topography on the plume as it meanders down the river valley and spreads out where the valley opens up toward the south. The dark lines in the particle distribution indicate topographical channeling. Figures IV-7 and 8 show the effect of the second wind reversal, establishing the southerly breeze, reversing the plume, and transporting the remainder of the "old" plume back over the source region.

V. COMPARISON OF RESULTS

Because of the inherent differences between a time-varying, three-dimensional model and a steady-state, unidirectional Gaussian plume model, direct comparison of concentration calculations for long distances was best obtained by isopleths overlays.

Figs. V-1 to V-3 show the 24 h time-integrated, surface air concentration isopleths for the two radionuclides and the inert gas. Figure V-4 shows the surface deposition isopleths. The irregular contour lines are the ADPIC calculations; Gaussian results are either the sector-averaged radial arcs

between the dotted lines or the oval-shaped patterns. (Except for those contours to the west, the CPS contours have been sector-averaged over 22.5°). Isopleths for the 24 h integrated surface-air concentration are in s^2/m^3 at a height of 2 m above the topography. Isopleths for deposition are in s/m^2 and, when applicable, reflect continued radioactive decay on the ground.

The Gaussian patterns clearly show the two main meteorological regimes for the 24 h period. Isopleths toward the south-southwest result from the stable nighttime drainage wind and those to the north-northeast are from the neutral to unstable daytime breeze. In addition, there is one fan of Gaussian contours toward the west that represents the hourly average of the transition period when the wind changed direction.

The Gaussian model predicts higher concentrations along plume center lines than does the ADPIC model but these high values cover considerably less area. We expected to find this trend because the Gaussian model integrates a set of stationary plumes of infinite extent, thus calculating a contribution in areas where the pollutant never reached. An example of this is the westerly plume resulting from the period of wind shift from northerly to southerly. ADPIC contours in this direction indicate concentrations of several orders of magnitude less. The high cliffs on the east bank of the river and the transitory nature of the wind prevented the bulk of the pollutant from reaching the distances indicated by the Gaussian model during the wind shift period. Also, the presence of surface air pollutants over a much larger area as shown by the ADPIC contours is the result of exposure from the returning diffuse, secondary pollutant caused by the shifting and reversals of the wind during the 24 h period. This feature is not considered by the Gaussian model.

The greatest difference between the two models manifests itself under the stable nighttime drainage regime that gives rise to the south-southwesterly plume contours. Here, the Gaussian model exhibits integrated centerline concentrations much higher than those of ADPIC. The Gaussian formula predicts infinite concentrations as the mean wind $\bar{u}$ goes to zero. For stable conditions in this study, the mean wind near the surface was $\bar{u} < 0.5$ m/s, a value that is very close to this singularity. Consequently, very high concentrations were calculated by the Gaussian model.

An equally important difference between the models arises from the influence exerted on them by the topography. The ADPIC contours clearly exhibit the channeling effect of the river valley on the wind but the simple Gaussian model, because it is based on the local mean wind at the source only, does not account for this effect. This again is illustrated by the direction of the south-southwest nighttime Gaussian plume.

The above discussion applies to all figures V-1 to V-3. Figure V-4 presents the deposition isopleths for ^{131}I, the only species that had a deposition velocity of 0.005 m/s. Once again, the preceding discussion applies with the additional observation that most of the material is deposited near the source as might be expected for a surface release. The only other region of high deposition is a ridge on the east bank of the river, south of the source.

It is important to observe that the Gaussian model concentrates the total pollutant for the 24 h in discrete plumes while the ADPIC model spreads the pollutant over the entire area, corresponding to the time and space variability of the winds. This explains why the Gaussian centerline concentrations are always higher than the ADPIC contour values.

VI. CONCLUSIONS

Three-dimensional, time-dependent PIC model calculations exhibit several advantages over steady state Gaussian models for assessment calculations. PIC models more closely simulate the three-dimensional physical processes of the planetary boundary layer. This appears clearly when sites with strong individual topographic and meteorological features are considered. The Hudson River Valley is an area in which the local topography at times can strongly influence the day and nighttime meteorological regimes. Under these circumstances, the results of the PIC and Straight-Line Airflow Gaussian methods differed greatly. Overall, the Gaussian method calculated higher concentrations under stable conditions; agreement between the two methods was better for neutral to unstable conditions. The PIC method calculated air concentrations over larger areas than did the Gaussian model, because of its inclusion of meandering and secondary exposure from the returning plume after flow reversal.

For this study, the 24 h runs were used to draw a comparison between the two methods for estimating air concentration and deposition. To determine if these differences persist for longer periods of time, we are presently developing techniques for yearly assessments calculated economically with the PIC method.

1. K. R. Peterson, T. V. Crawford, and L. A. Lawson, "CPS: A Continuous Point Source Computer Code for Plume Dispersion and Deposition Calculations," Lawrence Livermore Laboratory Report UCRL-50249 (1976).

2. D. H. Slade, "Meteorology and Atomic Energy," Energy Research and Development Administration Report TID-24190 (1968).

3. C. A. Sherman, "A Mass-Consistent Model for Wind Fields Over Complex Terrain," Lawrence Livermore Laboratory Report UCRL-76161 Rev. 2 (1976). Submitted to the *Journal of Applied Meteorology*.

4. C. A. Sherman, "MATHEW: A Mass-Consistent Wind Field Model," Ph.D. thesis, University of California, Davis, CA, to be published.

5. R. Lange, "ADPIC - A Three-Dimensional Computer Code for the Study of Pollutant Dispersal and Deposition Under Complex Conditions," Lawrence Livermore Laboratory Report UCRL-51462 (1973).

6. R. Lange, "ADPIC - A Three-Dimensional Transport-Diffusion Model for the Dispersal of Atmospheric Pollutants and Its Validation Against Regional Tracer Studies," Lawrence Livermore Laboratory Report UCRL-76170 Rev. 2 (1976). Submitted to the *Journal of Applied Meteorology*.

7. P. H. Gudiksen, K. P. Peterson, R. Lange, and J. B. Knox, "Plume Depletion Following Postulated Plutonium Dioxide Releases from Mixed-Oxide Fuel-Fabrication Plants," Lawrence Livermore Laboratory Report UCRL-51781 (1975).

8. Preliminary Safety Analysis Report for Indian Point Nuclear Generating Unit No. 3," Con-Edison Co. of New York (1973).

Table 3.1. Elemental species used in model calculations.

Species	Half-life (s)	Deposition velocity (m/s)
^{131}I	6.91×10^5	0.005
^{138}Xe	8.40×10^2	-
Inert gas	∞	-

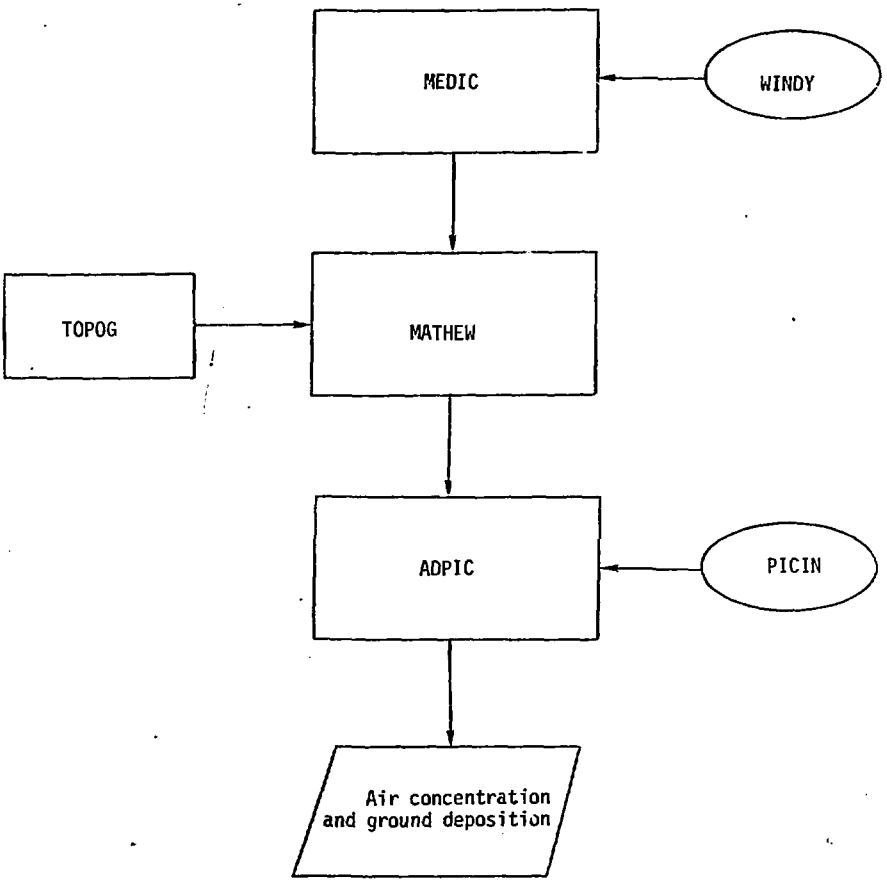

Fig. II-1. Schematic diagram of model components for the PIC method.

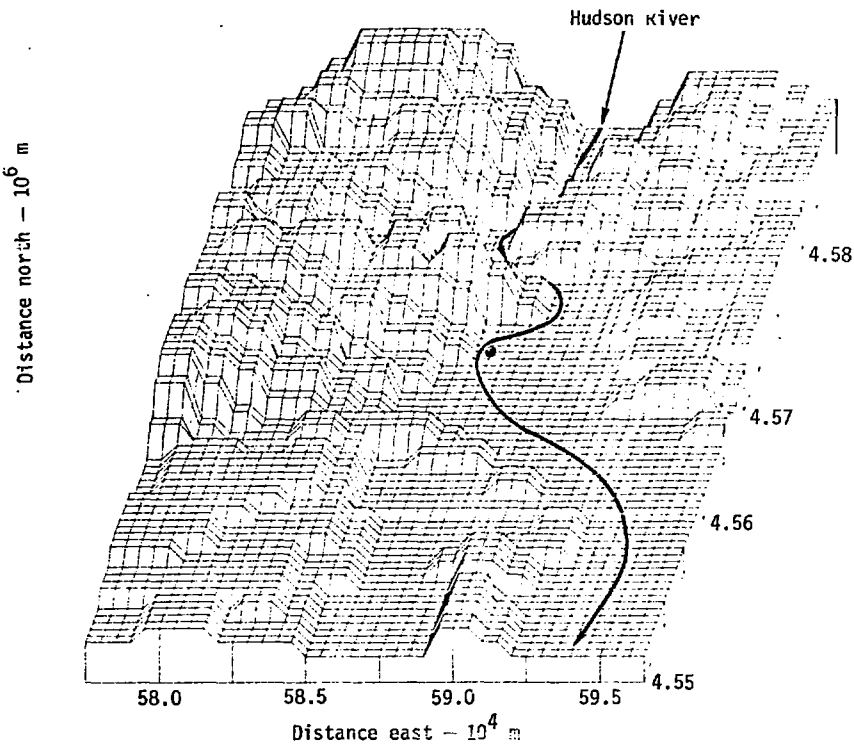

Fig. III-1. Computer generated topography (MATHEW) for the Hudson River Valley. Source is located by (●).

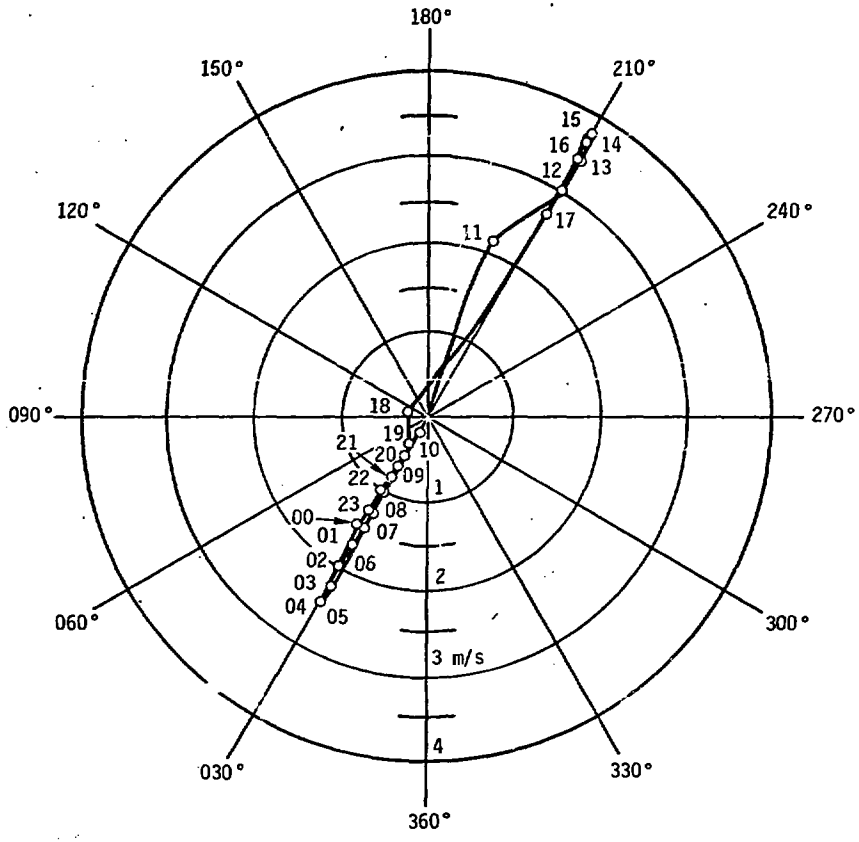

Fig. III-2. Assumed variation of mean wind-vector speed (m/s) for a 24-h period in the Hudson River Valley.

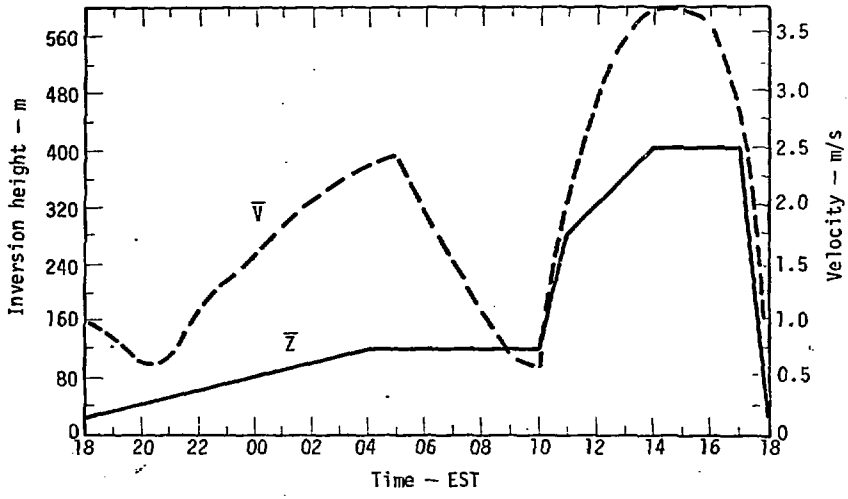

Fig. III-3. Assumed variation of mean wind speed ($\bar{V}$) and height of inversion base ($\bar{Z}$) vs time of day for the Hudson River Valley.

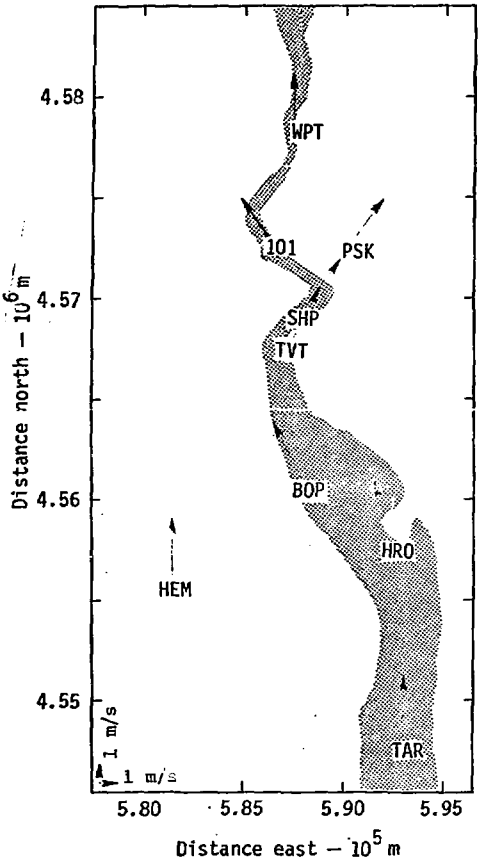

Fig. IV-1. Assumed surface-wind measurements at 1200 EST in the Hudson River Valley. Locations: BOP, Bowline Point; HEM, Hempstead; HRO, Hudson River; IOI, Iona Island; PSK, Peekskill; SHP, Ship; TAR, Tarrytown; TVT, Indian Point; WPT, West Point.

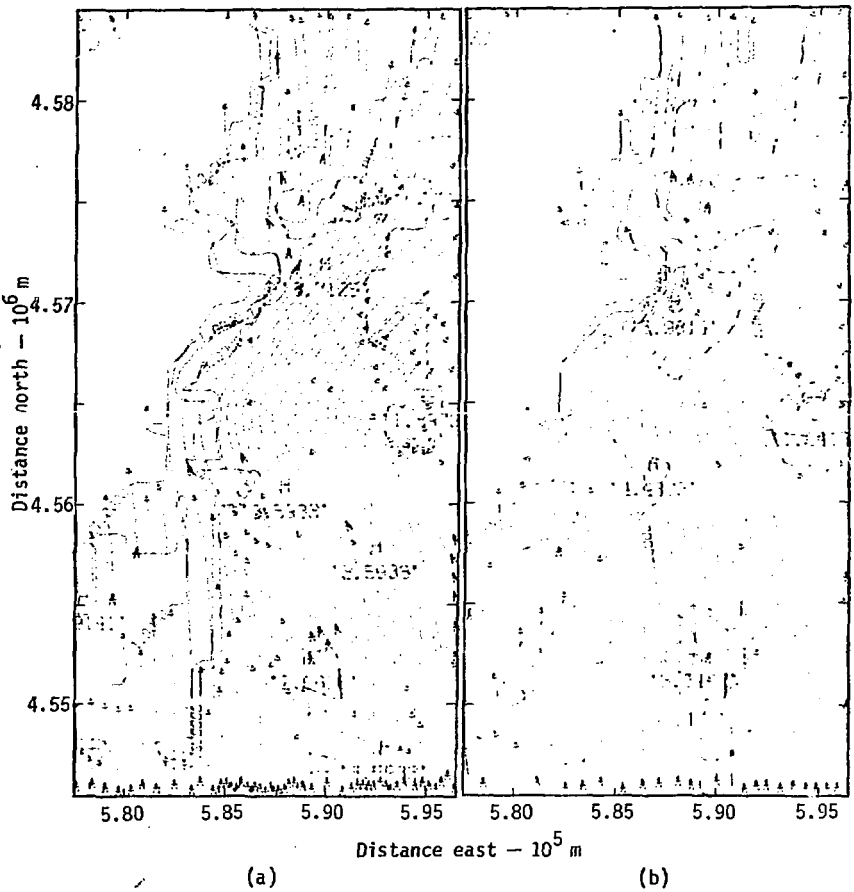

Fig. IV-2. Interpolated (a) and adjusted mass-consistent (b) horizontal wind field (m/s) at 1200 EST in the Hudson River Valley 90 m above the lowest topography in the grid.

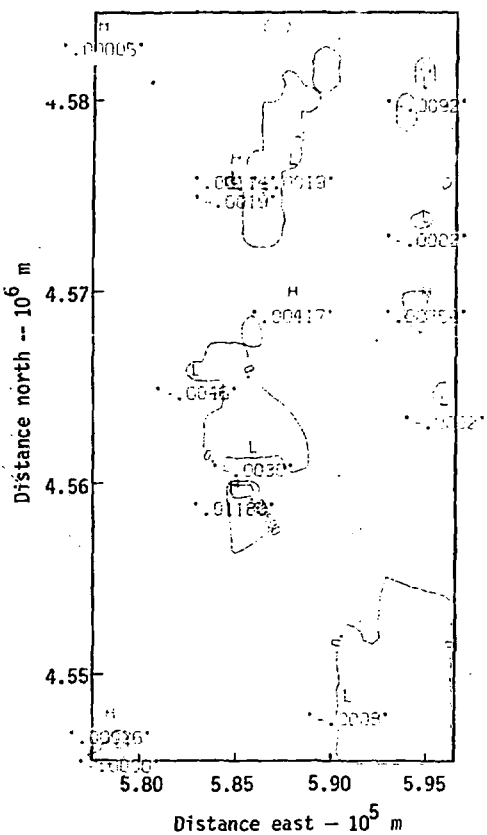

Fig. IV-3. Vertical velocity contours (m/s) at 1200 EST in the Hudson River Valley.

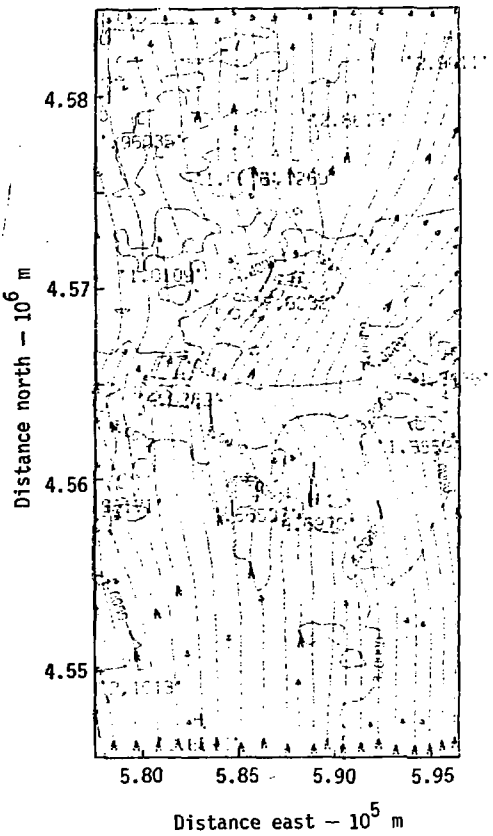

Fig. IV-4. Adjusted wind field (m/s) 45 m above the topography at 1200 EST in the Hudson River Valley.

Fig. IV-5. ADPIC particle plume during the onset of the nighttime drainage regime in the Hudson River Valley: 2200 EST.

Fig. IV-6. ADPIC particle plume during the nighttime drainage regime in the Hudson River Valley: 0100 EST.

Fig. IV-7
1200 EST

ADPIC particle plume during the afternoon southerly breeze in the Hudson River Valley.

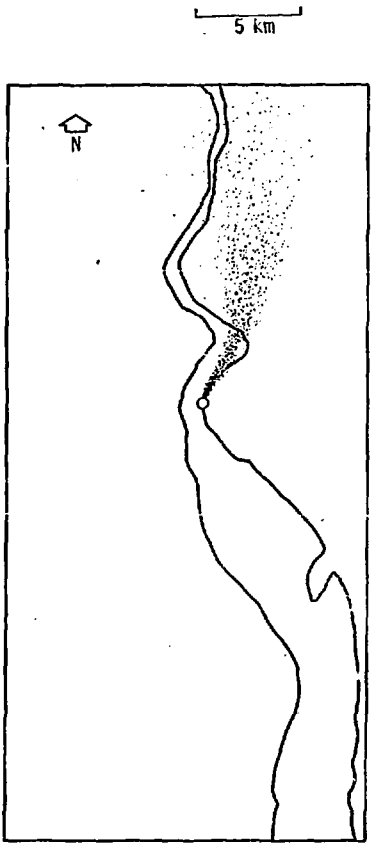

Fig. IV-8
1700 EST

ADPIC particle plume during the afternoon southerly breeze in the Hudson River Valley.

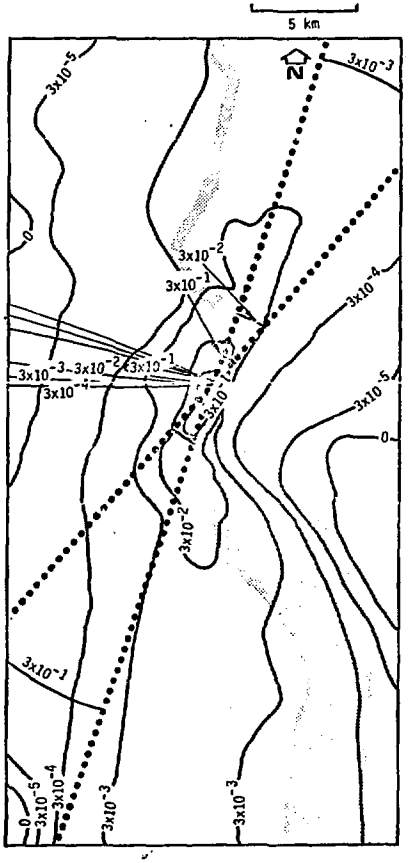

Fig. V-1. Relative surface-air concentration isopleths for inert gas.

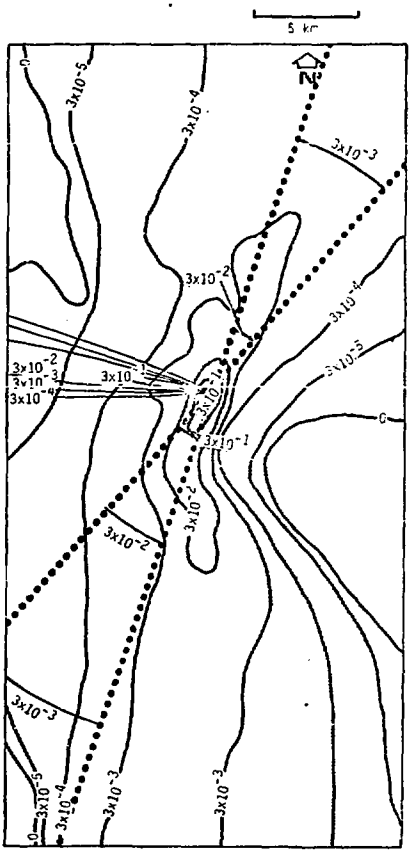

Fig. V-2. Relative surface-air concentration isopleths for ^{131}I.

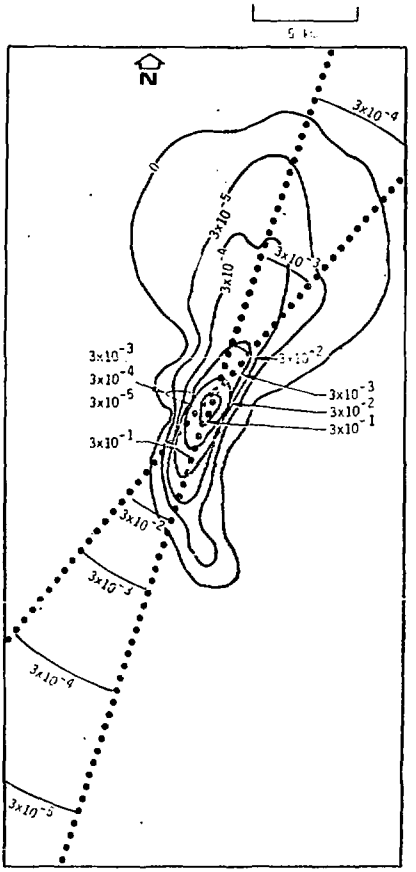

Fig. V-3. Relative surface-air concentration isopleths for ^{138}Xe.

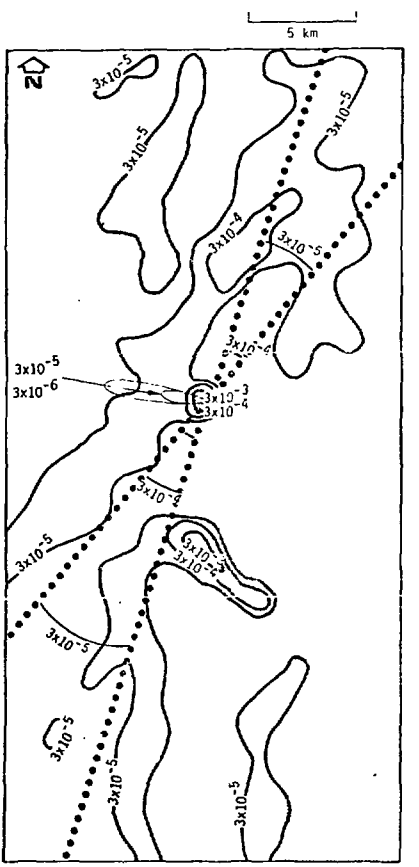

Fig. V-4. Relative ground deposition isopleths for ^{131}I.